

Dalton Transactions

Accepted Manuscript



This is an *Accepted Manuscript*, which has been through the Royal Society of Chemistry peer review process and has been accepted for publication.

Accepted Manuscripts are published online shortly after acceptance, before technical editing, formatting and proof reading. Using this free service, authors can make their results available to the community, in citable form, before we publish the edited article. We will replace this *Accepted Manuscript* with the edited and formatted *Advance Article* as soon as it is available.

You can find more information about *Accepted Manuscripts* in the [Information for Authors](#).

Please note that technical editing may introduce minor changes to the text and/or graphics, which may alter content. The journal's standard [Terms & Conditions](#) and the [Ethical guidelines](#) still apply. In no event shall the Royal Society of Chemistry be held responsible for any errors or omissions in this *Accepted Manuscript* or any consequences arising from the use of any information it contains.

ARTICLE

Ligand-based Photooxidations of Dithiomaltolato Complexes of Ru(II) and Zn(II): Photolytic CH Activation and Evidence of Singlet Oxygen Generation and Quenching

Cite this: DOI: 10.1039/x0xx00000x

Received 00th January 2012,
Accepted 00th January 2012

DOI: 10.1039/x0xx00000x

www.rsc.org/

Britain Bruner^a, Malin Backlund Walker^b, Mukunda M. Ghimire^c, Dong Zhang^c, Matthias Selke^c, Kevin Klausmeyer^a, Mohammad A. Omary^c, and Patrick J. Farmer^{*a,b}

The complex $[\text{Ru}(\text{bpy})_2(\text{ttma})]^+$ (bpy = 2,2'-bipyridine; ttma = 3-hydroxy-2-methylthiopyran-4-thionate, **1**), has previously been shown to undergo an unusual C-H activation of the dithiomaltolato ligand upon outer-sphere oxidation. The reaction generated alcohol and aldehyde products **2** and **3** from C-H oxidation of the pendant methyl group. In this report, we demonstrate that the same products are formed upon photolysis of **1** in presence of mild oxidants such as methyl viologen, $[\text{Ru}(\text{NH}_3)_6]^{3+}$ and $[\text{Co}(\text{NH}_3)_5\text{Cl}]^{2+}$, which do not oxidize **1** in the dark.

This reactivity is engendered only upon excitation into an absorption band attributed to the ttma ligand. Analogous experiments with the homoleptic $\text{Zn}(\text{ttma})_2$, **4**, also result in reduction of electron acceptors upon excitation of the ttma absorbance band. Complexes **1** and **4** exhibit short-lived visible fluorescence and long-lived near-infrared phosphorescence bands. Singlet oxygen is both generated and quenched during aerobic excitation of **1** or **4**, but is not involved in the C-H activation process.

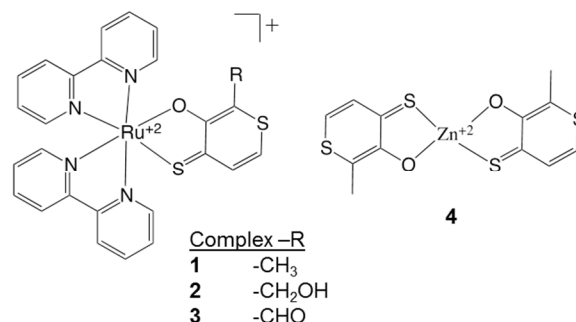
Introduction

Much effort has gone into the development of new photochemical dyes which induce electron transfer reactions upon exposure to light, for use in dye sensitized solar cell (DSSC) and other photochemical applications.¹ Most commonly used are luminescent compounds based on the well-known families of $\text{Ru}(\text{diimine})_x$ and porphyrin-based species, which form long-lived triplet states (³ES) that undergo facile electron-transfer reactions.² In particular, the $[\text{Ru}(\text{diimine})_2\text{L}]^{2+}$ family of complexes have been extensively studied due to photochemical redox reactivity involving electron transfer reactions from long-lived luminescent states.^{3–8}

Anthocyanin, a red dye found in many berries, was shown to have an unusually good efficiency as a DSSC dye when chelated to the surface of titania.⁹ Chemically similar hydroxy-pyrone chelates such as maltol have been studied for use as diagnostic tools,¹⁰ anticancer drugs,^{11,12} and metal transport.^{13–15} Thiomaltol,¹⁶ in which the pyronal ketone is replaced with a thione, has been used for similar

applications.^{17,18} A ring substituted derivative, 3-hydroxy-2-methyl-4H-thiopyran-4-thione, dithiomaltol or Httma, was first reported by Brayton, and displayed unusual aromaticity characterized by a downfield shift in the vinylic proton peaks in the ¹H NMR.¹⁹

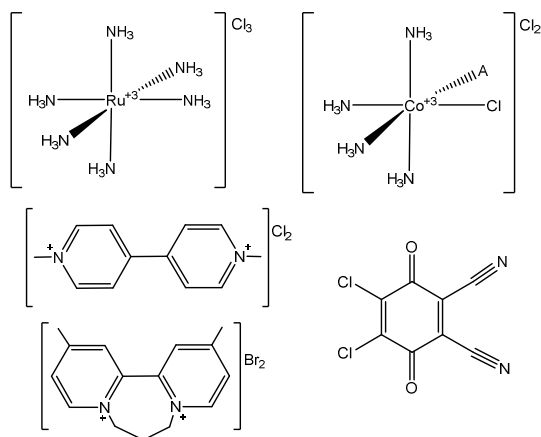
Scheme 1. Complexes investigated in this work.



Recently we reported that the bis-bipyridyl Ru complex of dithiomaltol, $[\text{Ru}(\text{bpy})_2(\text{ttma})][\text{PF}_6]$ or **1**, undergoes C-H activation

at a pendant alkyl position upon electrochemical or bulk oxidation, yielding $[\text{Ru}(\text{bpy})_2(\text{tma-alcohol})]^+$ **2** and $[\text{Ru}(\text{bpy})_2(\text{tma-aldehyde})]^+$ **3** as products, Scheme 1.²⁰ In this report we examine the photo-initiation of similar oxidative reactivity for compound **1** and the homoleptic $\text{Zn}(\text{tma})_2$ complex, **4**, using flash quench methodology,²¹ employing electron acceptors 4,4'-dimethyl-1,1'-trimethylene-2,2'-dipyridinium (DTDP²⁺), 1,1'-dimethyl-4,4'-bipyridinium (MV²⁺), $\text{Co}(\text{NH}_3)_5\text{Cl}^{2+}$, $\text{Ru}(\text{NH}_3)_6^{3+}$, and 2,3-dichloro-5,6-dicyano-1,4-benzoquinone (DDQ), Scheme 2.

Scheme 2. Oxidative quenchers used.



Results and discussion

Synthesis and characterization of Httma and $\text{Zn}(\text{tma})_2$, **4**.

Coordination complexes of Httma with metal ions are typically synthesized by deprotonation at room temperature or heating at high temperature in polar protic solvents.^{14,15} Both methods were used in synthesizing previously reported compounds $[\text{Ru}(\text{bpy})_2(\text{tma})][\text{PF}_6]$, **1**,²² and $\text{Zn}(\text{tma})_2$, **4**.²³ X-ray diffractometry was used to determine the structure of Httma, shown in Figure 1, and of **4** in Figure 2. Details of the crystal parameters, data collection, and refinement are summarized in Table 1. The structures of **1** and **3** were previously reported;²⁰ bond length data are compared in the Supplemental Materials.

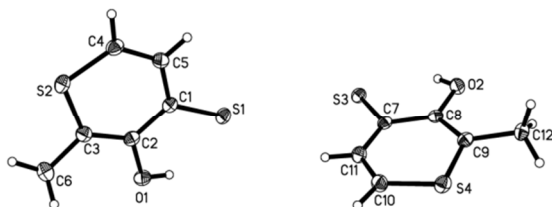


Figure 1. Crystal structure of Httma, two molecules are within the unit cell.

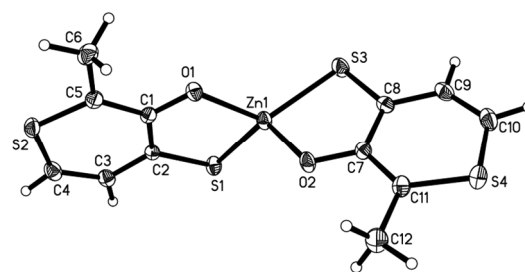


Figure 2. Crystal structure of $\text{Zn}(\text{tma})_2$, **4**.

Table 1. Crystallographic data

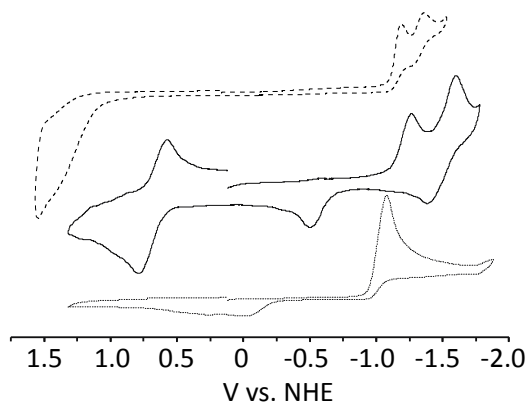
	Httma	4
Empirical formula	$\text{C}_6\text{H}_6\text{OS}_2$	$\text{C}_{13}\text{H}_{11}\text{Cl}_3\text{O}_2\text{S}_4\text{Zn}$
Formula mass	158.23	499.18
a (Å)	5.3629(4)	7.5568(9)
b (Å)	8.6723(7)	25.901(4)
c (Å)	13.5524(11)	7.6967(10)
α (°)	90.00	73.404(3)
β (°)	114.730(4)	79.141(3)
γ (°)	90.00	75.735(3)
V (Å ³)	1368.3(3)	921.33(16)
Z	8	2
Crystal System	Monoclinic	Triclinic
Space Group	P2(1)/c	P-1
T(K)	110(2)	110(2)
D_{calcd} (g/cm ⁻³)	1.536	1.536
μ (mm ⁻¹)	0.684	2.224
$2\theta_{\text{max}}$ (°)	28.3	28.32
Reflections measured	3347	4491
Reflections used	2983	3850
Data / restraints / parameters	2983 / 0 / 173	2850 / 0 / 210
R_1 [$I > 2\sigma(I)$]	0.0317	0.0383
wR_2 [$I > 2\sigma(I)$]	0.0757	0.0993
$R(F_o^2)$ (all data)	0.0366	0.0486
$R_w(F_o^2)$ (all data)	0.0799	0.1199
GOF on F_o^2	1.046	1.091

Table 2. Structural data of complex **4**.

Bond	(Å)	Angle	(deg.)
Zn(1)-O(1)	1.957(2)	O(1)-Zn(1)-O(2)	106.80(9)
Zn(1)-O(2)	1.979(2)	O(1)-Zn(1)-S(3)	123.38(6)
Zn(1)-S(3)	2.2871(8)	O(2)-Zn(1)-S(3)	88.79(6)
Zn(1)-S(1)	2.2968(8)	O(1)-Zn(1)-S(1)	89.48(6)
		O(2)-Zn(1)-S(1)	119.95(7)
		S(3)-Zn(1)-S(1)	129.30(3)

Ligand constraint in compound **4** distorts metal-centered geometry with O(1)-Zn(1)-S(3) angle at 123.38(6)° and O(2)-Zn(1)-S(3) at 88.79(6)°. The dihedral angle between the two ligands is 93° while the bite angles of the ligands are < 90°. Summary of selected bond lengths, angles, and interatomic distances for compound **4** are given in Table 2.

Electrochemical measurements. The ground state redox properties of Httma, **1** and **4** were assessed using cyclic voltammetry, shown in Figure 3 and Table 3. The Httma undergoes a characteristic irreversible reduction at -0.98 V NHE, with similar reductions seen at ca. -1.12 V for the metal complexes; a related oxidation wave is seen on the return scan, at ca. -0.1 V for Httma, and -0.4 and -0.6 V for compounds **4** and **1**, respectively. Compound **1** also displays quasi-reversible oxidation at 0.7 V, assigned to the Ru^{2+/3+} couple, and reduction at ca. -1.5 V, assigned to the bipyridine moieties.

**Figure 3.** Cyclic voltammograms of **1** (solid), **4** (dashed), and **httma** (dotted) in anhydrous CH₃CN with 0.1 M TBAPF₆ as the supporting electrolyte on glassy carbon disc electrode, scan rate 100 mV/s.**Table 3.** Electrochemical data.

	E ^o _{Ox}	E ^o _{Red}
Httma	-0.156(ir)	-0.969(ir)
1	+0.693	-1.117(ir)
		-1.488
4	+1.200(ir)	-1.119(ir)
		-1.359

All potentials adjusted vs. NHE in CH₃CN, 0.1 M TBAPF₆.

Photochemical characterizations. The normalized absorbance spectra of metal complexes **1**, **4** and well-known Ru(bpy)₃²⁺ are compared in Figure 4. The absorbance of metal-coordinated ttma is demonstrated by the band at 420 nm in the spectrum of Zn(ttma)₂, **4**. Several other ttma complexes show similar ligand-based absorbance bands with extinction coefficients on the order of 10 to 20 × 10³ L·mol⁻¹·cm⁻¹ per ttma ligand.²³ The spectrum of **1** shown exhibits mid-range bands from 450 to 750 nm which are significantly shifted and broadened in comparison to the analogous bands of [Ru(bpy)₃]²⁺. These and other determined photochemical properties of complexes **1** and **4** are given in Table 4.

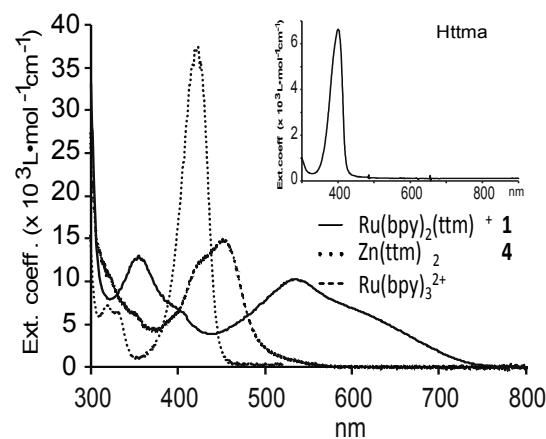
**Figure 4.** Comparison of normalized UV-vis spectra of [Ru(bpy)₂ttma]⁺ (—), Zn(ttma)₂ (•••) and Ru(bpy)₃²⁺ (---) molar extinction coefficient (L·mol⁻¹·cm⁻¹). Inset: of Httma over same range.

Table 4. Complex absorbance and emission data.

Complex	Absorbance max (nm)	Ext. coeff. ($M^{-1}\cdot cm^{-1}$)	Emission (nm)	Lifetime (μs)
1	352	16400	420 1080	0.01 8.50
	537	12100		
4	422	37100	450 1275	0.005 75.0

Excitation of **1** in CH_3CN solution at wavelengths > 400 nm generates no observable emissions, but excitation at 355 nm band obtains a short-lived fluorescence ($\lambda_{em} = 420$ nm, $\tau_{em} = 10$ ns) which increases in intensity ca. 100 fold at 77 K. Measurements in the near IR identified an emission at $\lambda_{em} = 1080$ nm with $\tau_{em} = 8.5$ μs , Figure 5.

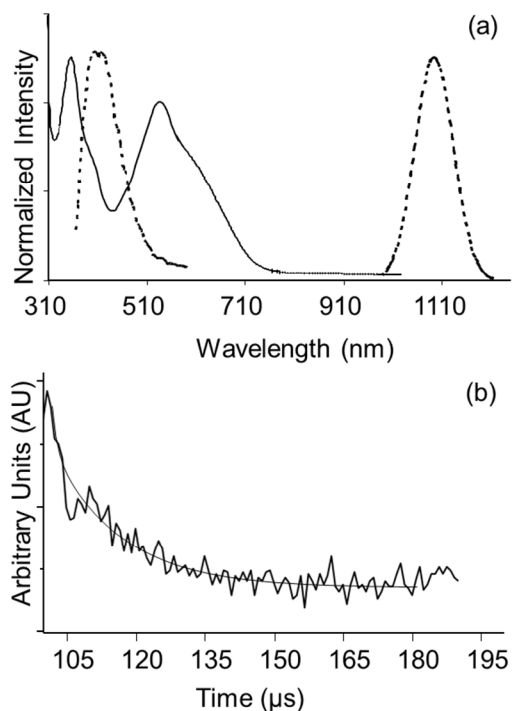


Figure 5. a) Normalized absorbance (solid line) and emission (dotted) spectra for compound **1** in CH_3CN . b) Emission transient trace from excitation at 352 nm, at 1080 nm ($\tau_{em} = 8.5$ μs).

Addition of MV^{2+} to anaerobic solutions of **1** significantly decreases the intensity of the 1080 nm emission (SM) but does not shorten its lifetime. Excitation of **4** into the 422 nm band ($\epsilon = 37100$ $M^{-1}cm^{-1}$) obtains a short lived ($\tau \sim 5$ ns) emission with maximum at 450 nm, which is quenched in the presence of excess of MV^{2+} .

Complex **4** has a phosphorescent emission at 1275 nm, $\tau_{em} = 75$ μs , Figure 6.

Bulk oxidations by flash quench photolysis. Initial flash quench experiments at room temperature showed that irradiation of **1** in CH_3CN/CH_3OH mixtures with a large 200-fold excess of the electron-acceptor methyl viologen, MV^{2+} , using a Hg lamp and a 400 nm low-pass filter generates a blue product solution characteristic of reduced MV^+ in ca. 15 min; addition of basic water to the product solution gives $[Ru(bpy)_2(ttma-alcohol)]^+$ **2** in ca. 10% yield by ESI-MS analysis, Figure 7.

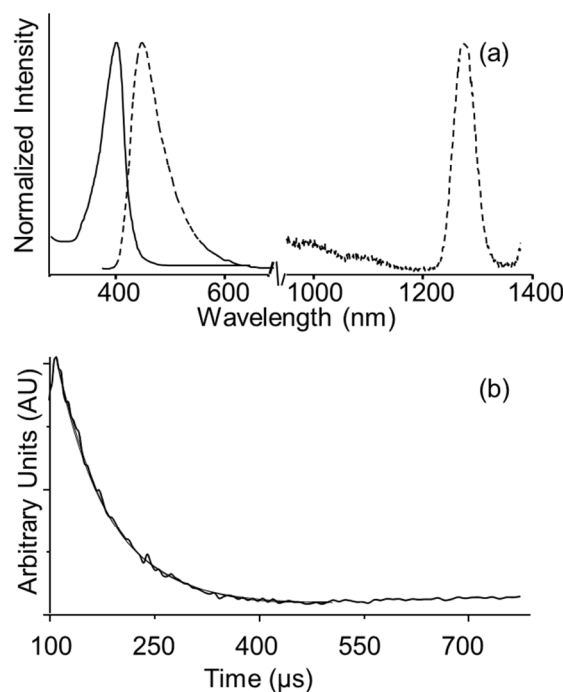


Figure 6. a) Normalized absorbance (solid line) and emission (dotted) spectra for **4** in CH_3CN . b) Emission transient trace at 1275 nm and data fit (dotted line, $\tau_{em} = 75$ μs), from excitation at 400 nm.

Analogous irradiation experiments using a 400 nm high-pass filter showed no observable changes. Photolysis of $[Ru(bpy)_2(ttma)]^+$ at room temperature in H_2O but in the absence of an electron transfer agent at room temperature leads to displacement of the ttma ligand to form the $[Ru(bpy)_2(H_2O)(OH)]^+$ complex, as previously reported for analogous complexes (Supplemental materials SM3).^{24,25} Subsequently, all photolysis experiments using complex **1** were conducted at 5 $^{\circ}C$ in the absence of water, with addition of basic water afterwards.

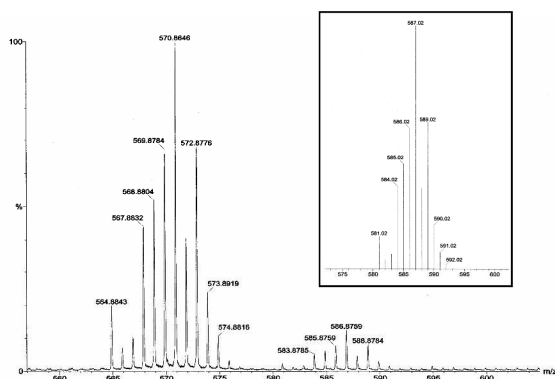


Figure 7. ESI-MS spectrum of a sample generated by photoexcitation of an anaerobic solution of $[\text{Ru}(\text{bpy})_2(\text{ttma})]^+$ and MV^{2+} in $\text{CH}_3\text{CN}/\text{CH}_3\text{OH}$ followed by the addition of 0.1 M NaOH. The species formed is $[\text{Ru}(\text{bpy})_2(\text{ttma-alcohol})]^+$ ($m/z = 587$). Inserted in the box is the predicted isotopic envelope for $[\text{Ru}(\text{bpy})_2(\text{ttma-alcohol})]^+$.

Bulk photolysis of CH_3CN solutions of **1** in the presence of varied potential electron acceptors $\text{Co}(\text{NH}_3)_5\text{Cl}_3$ and $\text{Ru}(\text{NH}_3)_6\text{Cl}_3$ generated color changes indicative of reduction of the oxidants; the reactions were quenched with the addition of basic water after photolysis. LCMS of the product solutions from these reactions after 20 minutes showed distinct retention times approximately 30 s apart for the complexes **1-3**, Figure 8. Selected ion monitoring (SIM) was used to assign Total Ion Current (TIC) peaks to the products separated.

Definitive characterization of the C-H oxidation products was obtained by chromatographic separations following analogous larger scale reactions over 3 hrs, Table 5. ^1H NMR characterization of the isolated **3** was used to confirm the structural assignment (Supplemental SM4) by comparison to the original reported spectra as well as to that of new samples of **3** generated by dark oxidation of **1** using the organic oxidant DDQ. Yields of the alcohol **2** were not obtained due to its decomposition during aerobic purification and manipulations.

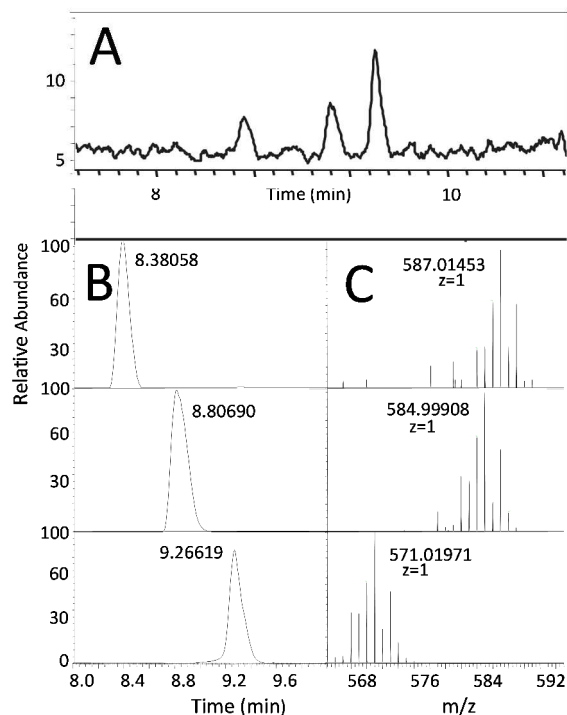


Figure 8. LCMS analysis of product solution after photolysis of **1** for in presence of $\text{Ru}(\text{NH}_3)_6\text{Cl}_3$ at 1:1.1 stoichiometry in CH_3CN . A) Region of the total ion current chromatogram showing product peaks; selective ion mass chromatogram peaks (B) and corresponding ion mass spectra ($m/z=1$) (C) of $[\text{Ru}(\text{bpy})_2\text{ttma-OH}]^+$, $[\text{Ru}(\text{bpy})_2\text{ttma=O}]^+$, and $[\text{Ru}(\text{bpy})_2\text{ttma}]^+$.

Table 5. Photolysis yields

Oxidant	% Yield ^a (Isolated ^b)		
	1	2	3
MV^{2+}	73 (61.4)	15	12 (7.15)
$\text{Ru}(\text{NH}_3)_6^{+3}$	45 (77.7)	9	34 (19.3)
$\text{Co}(\text{NH}_3)_5^{+3}$	45 (45.7)	16	39 (50.4)

^a LCMS yields using ca. 1.1 fold excess of oxidant, after 20 mins.

^b Isolated yields using ca. 1.4 fold excess oxidant, 200 fold for MV^{2+} , after 3 hrs.

Bulk photochemical oxidation of the homoleptic Zn complex **4** was assayed in a similar manner. Photolysis of **4** in the presence of DTDP^{2+} or MV^{2+} did not produce noticeable color changes indicative of irreversible reduction. Photolysis in the presence of $\text{Co}(\text{NH}_3)_5\text{Cl}$, $\text{Ru}(\text{NH}_3)_6\text{Cl}_3$ and DDQ initiated a change in color of the reaction mixtures indicating reduction of the oxidants. Analysis of the photolyzed solutions by MS showed a mixture of oligomeric $\text{C}_x\text{H}_y\text{O}_z^+$ species as the main components (Supplemental SM5); the

structures of these species have not been determined. The potential dependence of the oxidative flash quench yields are shown in Table 6. The trend in increasing $E^{0'}$ and yield across the photo-oxidants follows as $\text{Co(III)} > \text{Ru(III)} > \text{MV}^{+2} > \text{DTDP}^{2+}$.

Table 6. Reduction potential vs. photolysis yields

Oxidant	$E^{0'}$ (V NHE)	Yield (%)	Zn^{\ddagger} (+/-)
DTDP ²⁺	-0.691 ^{26a}	-	-
MV ²⁺	-0.440 ^{27b}	27	-
Ru(NH ₃) ₆ ³⁺	-0.159 ^{28c}	43	+
Co(NH ₃) ₅ Cl ²⁺	0.341 ^{28c}	55	+
DDQ	0.754 ^{29d}	-	+

[‡] Photoreduction by **4** indicated by +/-.

Singlet O₂ sensitization/desensitization. The near IR emissions of both **1** and **4** are quenched in the presence of ³O₂, generating ¹O₂. Figure 11 shows the near IR emission signals of **1** and **4** as well as longer lived emission due to the ¹O₂ generated. Extrapolating the time-resolved singlet oxygen emission signal to $t = 0$ yields a value of $\Phi^{\Delta} = 0.14 \pm 0.02$ for **1** and 0.64 ± 0.06 for **4** in CD₃OD, with C₆₀ and Rose Bengal used as references. The ground state of complex **1** also functions as an efficient quencher of singlet oxygen; in Figure 11, the lifetime of the singlet oxygen signal in MeOD is shortened from 170 μsec to 67 μsec due to quenching by ground-state [Ru(bpy)₂(tma)]⁺; the lifetime of singlet oxygen is unaffected by compound **4**. Additional data is given in Supplemental (SM7 and SM8) The total rate constant for removal of ¹O₂ by ground state complex **1** in CD₃OD was determined by time-resolved singlet oxygen luminescence quenching experiments to be $5.0 \pm 0.2 \times 10^8 \text{ M}^{-1}\text{sec}^{-1}$.

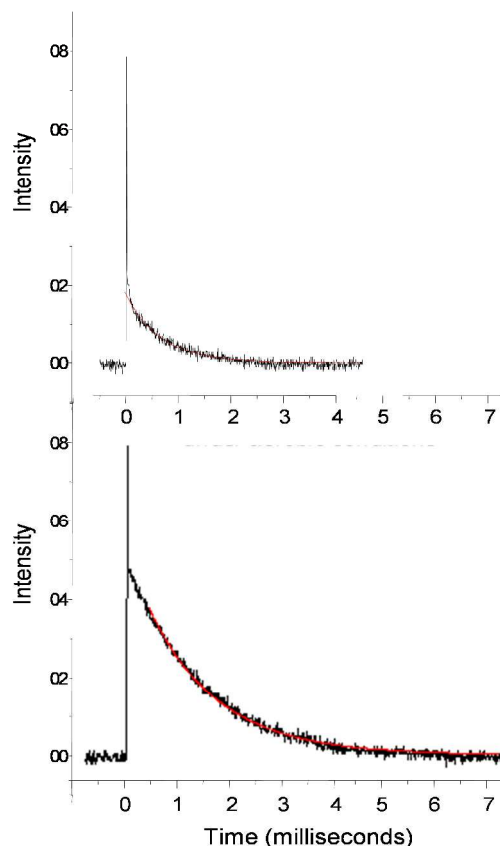


Figure 11. Singlet oxygen emission transient trace in near IR obtained upon excitation of **1** (top) and **4** (bottom) at 355 nm under aerobic conditions. The inset lines represent the best exponential fits for the long-lived emission due to singlet oxygen. The sharp emission peaks are due to the inherent emissions of the complexes.

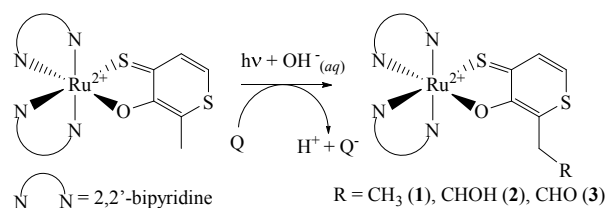
Discussion

Previous work demonstrated that bulk or electrochemical oxidation of **1** generated a darkly colored species, which reacted with water or other nucleophiles to give products oxidized at the pendant methyl. We noted that the ring proton resonances in ¹H NMR spectra of the Ru-bound tma suggest it to possess aromaticity. We rationalized the C-H oxidation as a result of thiopyrillium character in the oxidized tma ligand.^{24–36}

In this work we investigated the initiation of this oxidative chemistry by photo-excitation, analogous to the well-known flash-quench reactivity of Ru(bpy)₃²⁺.^{5,21} Our goal was to initiate the oxidation of **1** by flash quench methods, i.e. to excite the complex in the presence of an electron acceptor and look for the C-H oxidation products. No reactivity was seen upon excitation into the broad visible absorbance of **1**, but excitation with wavelengths below 400 nm did induce electron transfer reactivity, **Scheme 3**. Good yields of the same products formed by ground state oxidation were obtained

using high potential electron acceptors during flash-quench reactions.

Scheme 3. Oxidative quenching reaction



The MLCT-like absorbances of **1** are significantly broader than that of [Ru(bpy)₃]²⁺, suggesting strong electronic coupling between the Ru(II) and ttma ligand, but no analogous luminescence is obtained. We found excitation into a band tentatively assigned to the ttma ligand generates a short-lived singlet emission and a long-lived emission in the near IR, more characteristic of organic triplet phosphorescence. The homoleptic Zn complex **4** was used as a simple test of these assignments; and excitation of **4** into the analogous ttma band at 422 nm did indeed generate similar fluorescent and phosphorescent emissions. Photo-excitation of Httma alone yields no products, thus coordination to a metal center is essential for the observed electron transfer chemistry to take place.

The possible involvement of trace oxygen contamination was also investigated. Both compounds **1** and **4** are efficient sensitizers of singlet oxygen; compound **1** also functions as an efficient singlet oxygen desensitizer. These may be examples of singlet oxygen sensitization by a simple Forster mechanism, i.e. by an emission/absorbance overlap. Excitation of **1** under air generates no observable yields of the C-H activation products **2** or **3**, indicating that singlet oxygen itself is not involved in the C-H activation process, consistent with the known reactivity of ¹O₂.³⁰

Thus excitation of **1** produces a photostate which is capable of irreversibly reducing MV²⁺ (E⁰ = -440 mV NHE) but not DTDP²⁺, (E⁰ = -691 mV). This highly reducing photostate must be relatively short-lived, as any species capable of reducing MV²⁺ should quantitatively reduce both Ru(NH₃)₆³⁺ and Co(NH₃)₅Cl²⁺. Also notable is that an excess of MV²⁺ effectively quenches the emissions of the homoleptic Zn adduct **4** but does not irreversibly oxidize it, as occurs in analogous photolysis experiments with Ru(NH₃)₆³⁺ and Co(NH₃)₅Cl²⁺ quenchers. Thus complex **1** is a more powerful photo-reductant than **4**, roughly following the observed ground state

reduction potentials which are assigned to the ttma moiety in these species.

Scheme 4. Photochemical cycles based on triplet reactivity

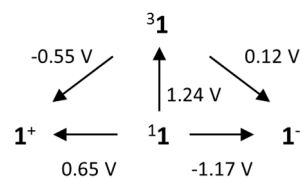


Table 7. Thermodynamic estimates for triplet energies

Complex	E ⁰⁰ (nm) ^a	E ⁰⁰ (eV)	E*Ox (V NHE)	E*Red (V NHE)
1	1000	1.24	-0.55	0.12
4	1220	1.02	0.18	-0.17

^a estimated from edge of emission band

A simple thermodynamic cycle denoting possible electron transfer reactions of the phosphorescent state of **1** is shown in Scheme 4, and comparable data for **4** is given in Table 7. The short-wavelength edges of the emissions were used to estimate the energy between the lowest triplet state and ground state.³¹ From these values, the excited state of **1** is predicted to be competent to reduce MV²⁺, while that of **4** is not and thus matching our results. But similarly, the triplet excited state of **4** should not reduce Ru(NH₃)₆³⁺, counter to experiment. As previously noted, the addition of MV²⁺ to anaerobic solutions of **1** prior to photo-excitation significantly decreases the intensity of the near IR emission without shortening its lifetime. This implies that once formed, the emissive state is not involved in the electron transfer, i.e., the photo-state which reduces MV²⁺ must precede the phosphorescent state.

Thus, the nature of the reductive excited states of compounds **1** and **4** remain obscure. Certain aromatic thiones demonstrate unusual phosphorescence,³²⁻³⁴ for example T₂ emissions have been described for uncomplexed aromatic thiones, as well as T₁-T₂ energy inversion caused by interactions of the excited state with solvent.³⁵⁻³⁷ A thione similar to Httma, 3-hydroxyflavothione demonstrates a long-lived emission when coordinated to transition metals with paired electrons,^{35,36} very similar to the behavior described here.

Experimental

Materials. The dithiomaltol ligand, $[\text{Ru}(\text{bpy})_2(\text{ttma})]\text{PF}_6$, $\text{Zn}(\text{ttma})_2$ and 4,4'-dimethyl-1,1'-trimethylene-2,2'-dipyridinium dibromide, $(\text{DTDP})\text{Br}_2$, were prepared according to published procedures.^{22,23} Electron acceptors 1,1'-dimethyl-4,4'-bipyridinium dichloride $(\text{MV}^{+2})\text{Cl}_2$, $\text{Co}(\text{NH}_3)_5\text{Cl}_3$, $\text{Ru}(\text{NH}_3)_6\text{Cl}_3$, and 2,3-dichloro-5,6-dicyano-1,4-benzoquinone (DDQ) and all other chemicals used were purchased from Sigma-Aldrich. Air-sensitive manipulations were carried out using Schlenk techniques or in an anaerobic dry glovebox.

Physical measurements. UVvis spectra were recorded by Perkin Elmer Lambda 900 or a Hewlett Packard 8453 Diode Array spectrophotometers. Emission and excitation spectra were recorded on a Hitachi F-4500 fluorescence spectrometer. All photochemical reactions were performed anaerobically in anaerobic quartz fluorescence cells or sealed jacketed beakers.

Crystallographic data was collected on crystals with dimensions 0.31 x 0.18 x 0.08 mm for **1**, 0.28 x 0.17 x 0.14 mm for **2**, 0.28 x 0.17 x 0.14 mm for **4**, and 0.31 x 0.18 x 0.08 mm for Httma. Data was collected at 110 K on a Bruker X8 Apex using Mo- K radiation ($\lambda = 0.71073 \text{ \AA}$). All structures were solved by direct methods after correction of the data using SADABS.³⁷⁻³⁹ All the data were processed using the Bruker AXS SHELXTL software, version 6.10.⁴⁰

Redox potentials were measured by cyclic voltammetry under anaerobic conditions using a CHI-760B potentiostat in dry-degassed CH_3CN with 0.1 M tetrabutylammonium hexafluorophosphate (TBAPF_6) as the supporting electrolyte. The cells consisted of a glassy-carbon working electrode (3.0 mm dia.), a AgCl coated Ag reference wire, and a coiled Pt wire auxiliary electrode. Measured potentials were corrected using a ferrocene standard, with the Fc/Fc^+ couple set to 400 mV NHE.

Large-scale photolysis experiments were carried out using an Oriel Apex Quartz Tungsten Halogen Source with a 150 W Xe Arc Lamp and filter accessories. Samples were stirred under N_2 at 5°C for 3 hr. Smaller scale photolysis were performed anaerobically under N_2 at 5°C in a 3 mL anaerobic quartz fluorescence cells for 45 min and worked up on bench top.

Mass Spectra were collected from an Accela Bundle Liquid Chromatograph (LC) coupled to a Thermo Electron Linear Trap Quadrupole Orbitrap Discovery mass spectrometer (Orbitrap) using positive electrospray ionization (+ESI) or by Direct Infusion (DI) with +ESI Data were collected and processed using Xcalibur v.2.0.7

software. Standards for LC separation were used to calibrate reaction yields for compounds **1** and **3**. Isolated yields were carried out by column-chromatography inside a glove box. Samples were collected and stored under inert atmosphere, removed from the glovebox, dried under vacuum, and returned to the glovebox to record mass and prepare samples for ^1H NMR.

Near IR emissions were measured in acetonitrile (CH_3CN) with a Photon Technology International (PTI) QuantaMaster Model QM-4 scanning spectrofluorometer equipped with a 75-watt xenon lamp, emission and excitation monochromators, excitation correction unit, and a near-infrared (NIR) photomultiplier tube (PMT) from Hamamatsu. Lifetimes were collected using a pulsed Xenon source with a pulse repetition rate of 300 pulse/sec and a PTI-supplied Gated Voltage-Controlled Integrator to interface to the NIR PMT.

Synthesis of dithiomaltol, Httma. Dithiomaltol was synthesized using a modification of previously reported methods.⁹ A sample of 3-hydroxy-2-methyl-4-pyrone (maltol, 1.0 g, 7.93 mmol) was combined with 1.1 eq of hexamethyldisiloxane (HMDO, 1.85 mL, 87.2 mmol) in 60 mL of anhydrous toluene and gently heated for 30 min. A sample of Lawesson's Reagent (3.53 g, 87.3 mmol) was then added before fitting the reaction flask with a condenser, and heated to reflux under nitrogen for 1.5 h. A black precipitate was removed by vacuum filtration, and the filtrate was concentrated to give a dark brown solid. The product was purified by silica flash column chromatography eluting with 4% CH_3OH in CH_2Cl_2 , as a bright orange band. After removal of solvent by reduced atmosphere, an orange solid was isolated, which gave dithiomaltol as orange iridescent flakes. Yield: 70%. Slow evaporation of the solid in hexanes gave orange needles suitable for x-ray diffraction studies. ^1H NMR (500 MHz, CDCl_3): δ 9.34 (s, 1H), 8.17 (d, 1H), 7.51 (d, 1H) 2.49 (s, 3H); ESI MS: m/z , 159 ($[\text{M} + \text{H}]^+$); UV-vis: CH_3CN , ϵ_{max} (ϵ in $\text{L}\cdot\text{mol}^{-1}\cdot\text{cm}^{-1}$) 221 ($\epsilon = 4,300$), 285 ($\epsilon = 1,700$), 397 ($\epsilon = 6,600$).

Synthesis of $\text{Zn}(\text{ttma})_2$, **4.** Httma (0.097 g, 0.613 mmol) was added to 19 mL of a stirred 0.029 M NaOH in a CH_3OH solution turning it a red color. Five minutes later ZnCl_2 (0.040 g, 0.291 mmol) and 20 mL of DI H_2O was added to the stirred solution, a light yellow precipitates formed immediately, and the reaction was left to stir overnight. Filtering the reaction solution yielded 0.092 g (83%) of a yellow solid. The compound was crystallized in CH_2Cl_2 by slow evaporation to produce samples suitable for X-ray

diffraction. ^1H NMR (500 MHz, CDCl_3): δ 2.64 (s, 6 H, $-\text{CH}_3$), 7.58 (d, 2 H, $J = 9.1$ Hz), 8.43 (d, 2 H, $J = 9.1$ Hz). Electrospray MS: 401 ($[\text{M}+\text{Na}]^+$). Anal. Calcd. for $\text{H}_{10}\text{C}_{12}\text{S}_4\text{O}_2\text{Zn}$: C, 37.90; S, 33.76; H, 2.65. Found: C, 37.70; S, 33.66; H, 2.63.

Chemical oxidation of $[\text{Ru}(\text{bpy})_2\text{ttma}][\text{PF}_6]$ with DDQ. The complex $[\text{Ru}(\text{bpy})_2(\text{ttma})][\text{PF}_6]$ (4.21 mg, 5.87 μmol) and DDQ (1.33 mg, 5.86 μmol) were placed in a 50 mL flask with 10.0 mL anhydrous CH_3CN . The flask was sealed, degassed with N_2 . The reaction was stirred for 45 min before the addition of NaOH_{aq} (1 mol eq) after which the solvent was removed under N_2 purge and separated by column chromatography inside a glove box using alumina as the separation media and anhydrous acetonitrile as the eluent. The isolated yield of aldehyde **3** was 3.94 mg (91.9 %). ESI MS: m/z 584.99. ^1H NMR (500 MHz, CD_3CN): δ 9.96 (d, $J = 1.5$, Hz, 1H), 9.18 (d, $J = 5$, Hz, 1H), 8.56 (d, $J = 5$, Hz, 1H), 8.46 (d, $J = 7.21$, Hz, 1H), 8.44 (d, $J = 8.29$, Hz, 1H), 8.43 (d, $J = 9.21$, Hz, 1H), 8.32 (d, $J = 8.3$, Hz, 1H), 8.08 (d, $J = 8.02$, 1.3, Hz, 2H), 8.05 (d, $J = 9.3$, Hz, 1H), 7.96 (d, $J = 8.03$, 1.49, Hz, 1H), 7.88 (d, $J = 5.7$, Hz, 1H), 7.79 (d, $J = 7.99$, 1.4, Hz, 1H), 7.76 (d, $J = 9.3$, 1.5, Hz, 1H) 7.62 (d, $J = 7.3$, 1.25, Hz, 1H), 7.61 (d, $J = 6.07$, Hz, 1H), 7.58 (d, $J = 7.3$, 1.3, Hz, 1H), 7.3 (d, $J = 7.31$, 1.2, Hz, 1H), 7.13 (d, $J = 7.3$, 1.3, Hz, 1H).

Large scale photochemical oxidations of $[\text{Ru}(\text{bpy})_2\text{ttma}][\text{PF}_6]$ (1**) and of $\text{Zn}(\text{ttma})_2$ (**4**).** In a typical experiment, samples of $[\text{Ru}(\text{bpy})_2(\text{ttma})][\text{PF}_6]$ (34.9 mg, 48.8 μmol) and pentaminechlorocobalt(III) chloride, $\text{Co}(\text{NH}_3)_5\text{Cl}_3$ (13.0 mg, 51.9 μmol) were placed in a 50 mL jacketed flask with 10.0 mL anhydrous acetonitrile. The flask was sealed, degassed with N_2 , and cooled to 5°C with a circulating cooling bath. The reaction mixture was photolyzed for 45 min with a 400 nm low-pass filter before the addition of NaOH_{aq} (1 mol eq), after which the solvent was removed under N_2 purge and separated on an alumina column inside a glove box with anhydrous CH_3CN as eluent. The isolated yield of aldehyde **3** was 17.9 mg (50.4 %). ESI MS: m/z 584.99. ^1H NMR (500 MHz, CD_3CN): δ 9.96 (d, $J = 1.5$, Hz, 1H), 9.18 (d, $J = 5$, Hz, 1H), 8.56 (d, $J = 5$, Hz, 1H), 8.46 (d, $J = 7.21$, Hz, 1H), 8.44 (d, $J = 8.29$, Hz, 1H), 8.43 (d, $J = 9.21$, Hz, 1H), 8.32 (d, $J = 8.3$, Hz, 1H), 8.08 (d, $J = 8.02$, 1.3, Hz, 2H), 8.05 (d, $J = 9.3$, Hz, 1H), 7.96 (d, $J = 8.03$, 1.49, Hz, 1H), 7.88 (d, $J = 5.7$, Hz, 1H), 7.79 (d, $J = 7.99$, 1.4, Hz, 1H), 7.76 (d, $J = 9.3$, 1.5, Hz, 1H) 7.62 (d, $J = 7.3$, 1.25, Hz, 1H), 7.61 (d, $J = 6.07$, Hz, 1H), 7.58 (d, $J = 7.3$, 1.3, Hz, 1H), 7.3 (d, $J = 7.31$, 1.2, Hz, 1H), 7.13 (d, $J = 7.3$, 1.3, Hz, 1H). Analogous experiments were carried out with MV^{+2} and $\text{Ru}(\text{NH}_3)_6\text{Cl}_3$ as described in text.

Photochemical oxidations of $\text{Zn}(\text{ttma})_2$ follow the same procedures. As example, a mixture of **4** (12.6 mg, 33.0 μmol) and $\text{Co}(\text{NH}_3)_5\text{Cl}_3$ (7.4 mg, 41.3 μmol) were placed in a 50 mL jacketed flask with 25.0 mL anhydrous CH_3CN . The flask was sealed, degassed with N_2 , and cooled to 5°C with a circulating cooling bath. The reaction was photolyzed for 45 min with a 400 nm low-pass filter before the addition of NaOH_{aq} (1 mol eq). With formation of an insoluble red precipitate; the remaining solution was analyzed by ESI-MS. Analogous experiments were done with DDQ as described in text.

Small scale photochemical oxidations of **1 and **4**.** These followed procedures described above. A stock solution of $[\text{Ru}(\text{bpy})_2\text{ttma}][\text{PF}_6]$ was prepared from 17.0 mg (23.7 μmol) in 5.0 mL anhydrous acetonitrile (4.75 mM); a sample of this solution (220 μL , 0.924 μmol) was mixed with 200 equivalents of MV^{+2} (4.76 mg, 0.185 mmol) in a purged quartz cell and irradiated for 15 min with a 400 nm low-pass filter. The reaction was then mixed with excess NaOH (0.25 mL of 0.143 M) and examined by LCMS for characterization and quantification of products.

Conclusions

The dithiomaltol complexes **1** and **4** undergo photo-oxidation in the presence of electron acceptors, reactivity which stems from transitions localized on the ligand. These results suggest the use of dithiomaltol and hetero-substituted maltol derivatives for applications which require photo-induced electron transfers independent of redox-active metal ions.

Acknowledgements

This research was supported by the American Chemical Society (PJF PRF 51921-ND3) and NIH-NIGMS (MS 5SC1GM084776). MAO acknowledges support by the National Science Foundation (CHE-0911690; CMMI-0963509; CHE-0840518) and the Robert A. Welch Foundation (Grant B-1542). We thank Professors Jay Winkler and T.J. Meyer for helpful discussions.

Notes and references

^a Department of Chemistry and Biochemistry, Baylor University, Waco, Texas 76798

^b Department of Chemistry, University of California, Irvine, Irvine CA 92697

^c Department of Chemistry, University of North Texas, Denton, Texas 76203

^d Department of Chemistry and Biochemistry, California State University, Los Angeles, Los Angeles, CA 90032

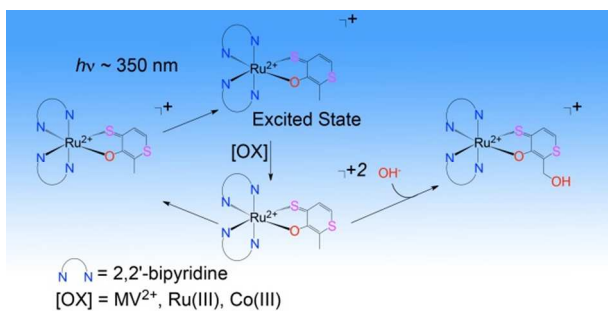
† This paper is dedicated to the memory of Prof. Oussama El-Bjeirami, who contributed to this work.

* Corresponding author. E-mail: Patrick_Farmer@baylor.edu (PJT).

Electronic Supplementary Information (ESI) available: including crystallographic data for Httma, 1H NMR comparison of compounds **1**, **3** and **4**, MS analysis of photolysis products, and steady state quenching and singlet oxygen quenching experiments. See DOI: 10.1039/b000000x/

References

- Robertson, N. *Angew. Chem. Int. Ed.* **2006**, *45*, 2338–2345.
- Huynh, M. H. V.; Dattelbaum, D. M.; Meyer, T. J. *Coord. Chem. Rev.* **2005**, *249*, 457–483.
- Durham, B.; Wilson, S. R.; Hodgson, D. J.; Meyer, T. J. *J. Am. Chem. Soc.* **1980**, *102*, 600–607.
- Collin, J.-P.; Jouvenot, D.; Koizumi, M.; Sauvage, J.-P. *Inorg. Chem.* **2005**, *44*, 4693–4698.
- Bjerrum, M. J.; Casimiro, D. R.; Chang, I. J.; Di Bilio, A. J.; Gray, H. B.; Hill, M. G.; Langen, R.; Mines, G. A.; Skov, L. K.; Winkler, J. R. *J. Bioenerg. Biomembr.* **1995**, *27*, 295–302.
- Hurst, J. K. *Coord. Chem. Rev.* **2005**, *249*, 313–328.
- Ghosh, P. K.; Brunschwig, B. S.; Chou, M.; Creutz, C.; Sutin, N. *J. Am. Chem. Soc.* **1984**, *106*, 4772–4783.
- Lebeau, E. L.; Adeyemi, S. A.; Meyer, T. J. *Inorg. Chem.* **1998**, *37*, 6476–6484.
- Cherepy, N. J.; Smestad, G. P.; Grätzel, M.; Zhang, J. Z. *J. Phys. Chem. B* **1997**, *101*, 9342–9351.
- Kandioller, W.; Kurzwernhart, A.; Hanif, M.; Meier, S. M.; Henke, H.; Keppler, B. K.; Hartinger, C. G. *J. Organomet. Chem.* **2011**, *696*, 999–1010.
- Hanif, M.; Schaaf, P.; Kandioller, W.; Hejl, M.; Jakupec, M. A.; Roller, A.; Keppler, B. K.; Hartinger, C. G. *Aust. J. Chem.* **2010**, *63*, 1521–1528.
- Enyedy, É. A.; Dömötör, O.; Varga, E.; Kiss, T.; Trondl, R.; Hartinger, C. G.; Keppler, B. K. *J. Inorg. Biochem.* **2012**, *117*, 189–197.
- Chaves, S.; Jelic, R.; Mendonça, C.; Carrasco, M.; Yoshikawa, Y.; Sakurai, H.; Santos, M. A. *Metallomics* **2010**, *2*, 220–227.
- Lewis, J. A.; Cohen, S. M. *Inorg. Chem.* **2004**, *43*, 6534–6536.
- Jacobsen, F. E.; Lewis, J. A.; Cohen, S. M. *J. Am. Chem. Soc.* **2006**, *128*, 3156–3157.
- Blazevic, K.; Jakopic, K.; Hahn, V. *Bull. Sci. Sect. Sci. Nat. Tech. Med.* **1969**, *14*, 1.
- Lewis, J. A.; Puerta, D. T.; Cohen, S. M. *Inorg. Chem.* **2003**, *42*, 7455–7459.
- Schlesinger, S. R.; Bruner, B.; Farmer, P. J.; Kim, S.-K. *J. Enzyme Inhib. Med. Chem.* **2013**, *28*, 137–142.
- Brayton, D.; Jacobsen, F. E.; Cohen, S. M.; Farmer, P. J. *Chem. Commun.* **2006**, 206.
- Backlund, M.; Ziller, J.; Farmer, P. J. *Inorg. Chem.* **2008**, *47*, 2864–2870.
- Chang, I. J.; Gray, H. B.; Winkler, J. R. *J. Am. Chem. Soc.* **1991**, *113*, 7056–7057.
- Backlund Walker, M. M. Unexpected reactivity of sulfur chelators. Ph.D., University of California, Irvine: United States -- California, 2009.
- Brayton, D. F. Targeting melanoma via metal based drugs: Dithiocarbamates, disulfiram copper specificity, and thiomaltol ligands. Ph.D., University of California, Irvine: United States -- California, 2006.
- Petroni, A.; Slep, L. D.; Etchenique, R. *Inorg. Chem.* **2008**, *47*, 951–956.
- Zhang, H.; Rajesh, C. S.; Dutta, P. K. *J. Phys. Chem. A* **2008**, *112*, 808–817.
- Alber, K. S.; Hahn, T. K.; Jones, M. L.; Fountain, K. R.; Van Galen, D. A. *J. Electroanal. Chem.* **1995**, *383*, 119–126.
- Frank, D. M.; Arora, P. K.; Blumer, J. L.; Sayre, L. M. *Biochem. Biophys. Res. Commun.* **1987**, *147*, 1095–1104.
- Curtis, N.; Lawrence, G.; Sargeson, A. *Aust. J. Chem.* **1983**, *36*, 1327–1339.
- Dileesh, S.; Gopidas, K. R. *J. Photochem. Photobiol. Chem.* **2004**, *162*, 115–120.
- Smitherman, H. C.; Ferguson, L. N. *Tetrahedron* **1968**, *24*, 923–932.
- Jonas, J.; Derbyshire, W.; Gutowsky, H. S. *J. Phys. Chem.* **1965**, *69*, 1–5.
- Saieswari, A.; Deva Priyakumar, U.; Narahari Sastry, G. *J. Mol. Struct. THEOCHEM* **2003**, *663*, 145–148.
- DeRosa, M. *Coord. Chem. Rev.* **2002**, *233–234*, 351–371.
- Murov, S. L.; Carmichel, G. L. *Handbook of Photochemistry*; CRC Press, 1993.
- Maciejewski, A.; Szymanski, M.; Steer, R. P. *Chem. Phys. Lett.* **1988**, *143*, 559–564.
- Szymanski, M.; Steer, R. P.; Maciejewski, A. *Chem. Phys. Lett.* **1987**, *135*, 243–248.
- Protti, S.; Mezzetti, A.; Cornard, J.-P.; Lapouge, C.; Fagnoni, M. *Chem. Phys. Lett.* **2008**, *467*, 88–93.
- Borges, M.; Romão, A.; Matos, O.; Marzano, C.; Caffieri, S.; Becker, R. S.; Maçanita, A. L. *Photochem. Photobiol.* **2002**, *75*, 97–106.
- Schindwein, W.; Waltham, E.; Burgess, J.; Binsted, N.; Nunes, A.; Leite, A.; Rangel, M. *Dalton Trans.* **2006**, 1313–1321.
- Sheldrick, G. M. *SHELXS97*; University of Gottingen, Germany, 1997.
- Sheldrick, G. M. *SHELXL97*; University of Gottingen, Germany, 1997.
- SAINT-Plus*; Bruker AXS Inc.: Madison, 2008.
- Sheldrick, G. M. *SHELXTL*; Bruker AXS Inc.: University of Gottingen, Germany, 2000.



Unusual light induced C-H oxidation initiated by excitation into Ru-bound dithiomaltol ligand absorbance.